Journal of Applied Polymer Science

Structure and properties relationship of melt reacted polyamide 6/malenized soybean oil

Juliano Roberto Ernzen,[1,2] Fabrício Bondan,[1] Caroline Luvison,[1] Cesar Henrique Wanke,[1] Johnny De Nardi Martins,[3] Rudinei Fiorio,[4] Otávio Bianchi[1]

[1]Programa de Pós-Graduação em Engenharia e Ciência dos Materiais-PGMAT, Universidade de Caxias do Sul, Rua Francisco Getúlio Vargas 1130, Bloco V, Caxias do Sul, Brazil

[2]Mantova Indústria de Tubos Plásticos Ltda, Caxias do Sul, Brazil

[3]Universidade Federal de Santa Catarina, Rua Pomerode 710, Campus Blumenau, Brazil

[4]Instituto Federal de Educação, Ciência e Tecnologia do Rio Grande do Sul, Rua Avelino Antônio de Souza 1730, Campus Caxias do Sul, Brazil

Correspondence to: Otávio Bianchi (E-mail: otavio.bianchi@gmail.com)

ABSTRACT: In this work, a maleinized soybean oil (SOMA) was melt reacted with polyamide 6 and the thermal, rheological, and morphological properties were evaluated. It was observed that the maleinized soybean oil reacted with polyamide chains, increasing the molecular weight of the polymer. Addition of SOMA also promoted an increase in the amount of α crystalline phase as well as in the crystallinity index. The average amorphous layer thickness (L_a) was enhanced with the addition of 1 wt % of SOMA, while the average crystalline layer thickness (L_c) were significantly enlarged with the increase in SOMA content, indicating that SOMA structures were located at the interfacial region between amorphous and crystalline. The addition of 5 wt % of SOMA plasticized the PA6, reducing its glass transition temperature. However, the sample containing 5 wt % of SOMA showed an accentuated pseudoplastic behavior as compared to other samples. Addition of SOMA also reduced the tensile strength and increased the elongation at break.
 J. Appl. Polym. Sci. **2016**, *133*, 43050.

KEYWORDS: blends; polyamides; properties and characterization; viscosity and viscoelasticity

Received 19 July 2015; accepted 14 October 2015
DOI: 10.1002/app.43050

INTRODUCTION

Several polymers require additives, such as plasticizers, flow agents, anti-UV, and antioxidants, among others. These additives can modify properties, such as chemical, mechanical, and rheological ones.[1–3] Additives and thermoplastic polymers have to be compatible in the development of new polymeric materials, which comply with the demands and industry requirements. Commonly, additives are derived from petrochemical sources.[4–7] However, many studies have been conducted aiming the use of renewable sources additives in new polymer formulations.[4–6,8,9] This trend is important by the search for less polluting alternative and innovation challenges in a field with relatively finite resources, such as petrochemical industry. Among additives from renewable sources, stands out those derived from plant oils such as carvacrol, cardanol, and soybean oils, which can be epoxidized and hydroxylated. These functional oils can be used as lubricants, plasticizers, and antibacterial agents.[4]

Polyamide 6 (PA6) is an engineering thermoplastic with high mechanical strength, high elastic modulus, and it can preserve its mechanical properties at elevated temperatures. Functional additives may be added to PA6 in order to achieve the desired properties for applications, such as hoses, containers, bumpers, frames, among others.[10–12] The compatibility between an additive of any kind and a polymer is a very important factor that often determines final applications.[7,13] Several parameters such as hydrogen bonding density, dielectric constant, and solubility parameter are used to quantify the level of interaction between polymer and additive.

In systems using plasticizers, for instance, when there are favorable chemical interactions, a plasticizer has a better ability to solvate the polymer chains. However, low molecular weight molecules migrate and can offer risks to human health, as is the case of dioctyl phthalate (DOP), a commonly used plasticizer in poly (vinyl chloride) formulations.[7] The use of alternatives

Additional Supporting Information may be found in the online version of this article.

plasticizers, like molecules from renewable and environmentally friendly natural sources, can be very interesting.[3] Molecules like soybean oil, castor oil, and tung oil are used for a long time and large scale in petrochemical field, but the physical–chemical interactions of these species often limit their use as additives for polymers. Aiming to improve the compatibility between polymers and additives, insertions of specific functional groups on renewable source molecules allow them react or form secondary bonds with polymers.[14,15] Soybean oil (SO) can be easily modified with maleic anhydride through Diels–Alder reactions.[16,17] Soybean oil modified with maleic anhydride (SOMA) can react specifically with polyamides and consequently be a very good alternative as a renewable source additive.

Reactive melt blending is a widely used technique in the modification and synthesis of polymers since early 1950. Polymer modification in a molten state involves reactions between a polymer, a monomer, and/or other reactive species.[18] These reactions purpose the formation of grafts in the main chain of the polymer, and thus change in macroscopic properties or promote compatibilization in immiscible systems.[18,19] This type of reaction is generally initiated by free radical generation by means of organic peroxides, azo compounds, etc.[20]

Polyamides can be chemically modified using reactive processing with the insertion of branchings. These modifications results in changes in melt temperature, reduction of half life crystallization time, and melt viscosity.[21,22] Reactions between bi and tri functional acids with polyamides result in reduction of melt viscosity without loss of mechanical properties. This is due to a balance between the polymer branches fraction regarding total molecules. Commercially polyamides can be modified with diester of carbonic acid, such diphenyl carbonate and dimethyl carbonate in presence of a specific catalyst.[23] Undoubtedly, the change of polyamide in castings state represents an interesting alternative; however, many aspects must be taken into account, such as possible degradation reactions and properties deterioration. Melt modification of PA using free radical reactions can results in molecular weight decrease with formation of aldehyde, azomethine, or unsaturated terminal groups as well as material yellowing.[21,22,24–28] Polyamides have terminal groups (—NH_2 and —COOH) which can react with anhydrides, for example. This approach is commonly used to decrease interfacial tension in immiscible polymer blends with PA with *in situ* copolymer formation. During the melt reaction with anhydrides, two mechanisms are proposed in literature. The first one is the reaction of an anhydride molecule with amino groups, and the second possibility is the reaction between amide and anhydride that result in chain scission. Both reaction possibilities modify the amino and carboxyl and group concentration and chain length.[22,23,25,29]

In this context, this work aims to correlate the mechanical, thermal, morphological, dynamic mechanical, and rheological properties of polyamide 6 (PA6) melt reacted with soybean oil chemically modified with maleic anhydride (SOMA). The PA6 and SOMA were blended by reactive melt extrusion. Evidence about the reaction of soybean oil chemically modified with maleic anhydride grafted on the PA6 chains with the amino polyamide terminal groups to produce long-branched macromolecules are reported.

EXPERIMENTAL

Materials

The polyamide 6 (RADILON S40F) used in this work have a density of 1.14 g cm^{-3} and a viscosity index (in sulfur acid) of 245 mL g^{-1}. A commercial soybean oil was used (Soya, Brazil), with acid number of 1.16 mg KOH g^{-1}. A maleic anhydride (PETROM) with total acid of 99.88 wt % was purchased from Mogi das Cruzes Petrochemistry S.A. The dicumyl peroxide (DCP) (98%, Sigma-Aldrich) was used as free radical initiator. All chemicals were used as received and without any further purification.

Methods

Maleinized Soybean Oil (SOMA). Soybean oil (600 g, 0.698 mol, assuming an average molecular weight of 870 g mol^{-1}) was placed in a round-bottom flask equipped with magnetic stirrer (1600 rpm) and thermometer. Maleic anhydride (135.1 g, 1.389 mol) was added and the mixture was maintained at 130°C for 90 min. Dicumyl peroxide (0.01 wt %) was used as free radical initiator of soybean oil modification. The color of solution changed from yellow to orange after 30 min. of reaction. At the end of 90 min, the solution became reddish and the viscosity increased. This reaction was done based on literature.[16,17] FTIR and ^{1}H NMR analysis showed that small content of maleic anhydride was left in the reaction medium. The FTIR spectra were performed on a Perkin-Elmer Impact 400 spectrometer in the attenuated total reflection (ATR) mode. The spectra were obtained over the 4,000 to 500 cm^{-1} region employing 32 scans with a resolution of 4 cm^{-1}. The ^{1}H NMR spectra for the samples were obtained on a Bruker Fourier 300 spectrometer. The ^{1}H NMR spectra were acquired from a chloroform-d solution with a sample concentration of 3 wt % at 22 °C.

FTIR-ATR: 3009 cm^{-1} (C═C); 2924, 2854, 1463 cm^{-1} (C—H); 1851, 1780, 888 cm^{-1} (O═C—O—C═O); 1238, 1161, 1057 cm^{-1} [C—C(═O)—O]; 1742 cm^{-1} (C═O).

^{1}H-NMR (CCl_4)δ: 0.84 (CH_3—); 1.22 (—CH_2—); 2.25 [—CH_2—C(═O)—O]; 2.7 (—CH═CH—$\underline{CH_2}$—CH═CH—); 3.1 [—CH—$\underline{CH}$— (CH_2—)—C(═O)]; 4.1 [—O—CH_2—$\underline{CH}$(O—)—CH_2—O—]; 4.2 [—O—$\underline{CH_2}$—CH(O)—] and 5.3 (—HC═CH—).

Melt Processing. PA6/SOMA reactive melt blends with different content of SOMA (1 and 5 wt %) were prepared in a modular MH Equipamentos (*L*/*D* 32) intermeshing corotating twin-screw extruder. The screw configuration employed comprises two staggered kneading blocks separated by a conventional conveying section. The set upstream contained dispersive and distributive elements as show in Figure 1. Barrel temperature was set at 230–260°C and the screws rotation was 50 rpm.

After melt processing, the samples were dried and injection-molded in a Battenfeld Plus 350/075 machine at a holding pressure of 500 bar and barrel temperature of 230°C with a Type I specimen mold according to ASTM D 638-08. The temperature of the injection mold was 80°C.

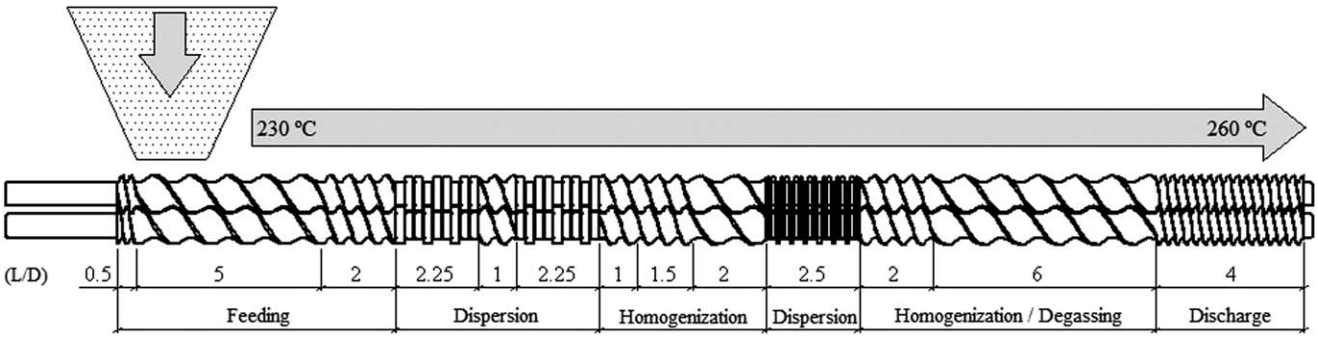

Figure 1. Screw profile.

Selective Extraction. Selective extraction was used to determine the amount of unreacted SOMA during reactive melt processing. After extrusion, samples were dried at 105°C during 24 h, placed in a 120-mesh wire cage containing approximately 0.3 g of polymer and maintained in a round-bottom flask containing boiling hexane for 8 h. After solvent extraction all samples were dried at 105°C for 12 h. The mass ratio obtained from the weights before and after extraction of the samples was used to determine the amount of unreacted SOMA.

Amine End Chain and Carboxyl Concentration. The amine end chain concentration was measured by titration. About 0.3 g of sample was dissolved in 20 mL of *m*-cresol at 190°C. The titrating solution was a methanol/water (75/25 v/v) 0.01*M* in HCl. The equivalence point was shown to be reached when a methyl yellow indicator turned reddish.[25]

Carboxyl end concentration was measured by titration. About 3 g of sample was dissolved in 750 mL of benzyl alcohol at 185°C. The samples were titrated with an ethanolic solution of NaOH (0.1*M*). The equivalence point was shown to be reached when a phenolphthalein indicator turned pink.[2]

Viscosity Number and Molecular Weight. The solution viscosity of the PA6/SOMA samples was measured with an Ubbelhode viscometer with formic acid according to ISO 307 standard. The intrinsic viscosity ($[\eta]$) of the samples was estimated using the Solomon–Ciuta equation of a single-point measurement[30,31]:

$$[\eta]=\frac{\left[2(\eta_{sp}-ln\eta_r)\right]^{0.5}}{c} \quad (1)$$

where η_{sp} is the specific viscosity, η_r is the relative viscosity, and C is the concentration (0.005 g mL^{-1}). The molecular weight (M_v) of the samples were estimated from $[\eta]$ values with the Mark–Houwink–Sakurada equation[32]:

$$[\eta]=K(M_v)^{\alpha} \quad (2)$$

where K and α are 0.023 mL g^{-1} and 0.82, respectively, for PA6 at 25°C in formic acid solution (85%).[24]

Differential Scanning Calorimetry (DSC). DSC analyses were performed in a DSC 50 Shimadzu using 9–10 mg of each sample under nitrogen atmosphere with a flow rate of 50 mL min^{-1}. The melting temperature and enthalpy were calibrated with Indium (T_m In = 156.6°C; ΔH_m In = 28.5 J g^{-1}). The samples were heated at 10°C min^{-1} to 280°C, and held at this temperature for 5 min to erase previous thermal history. The samples were then cooled to room temperature at 10°C min^{-1}.

Wide Angle X-ray Diffraction (WAXD). The WAXD analysis of the samples was performed in a Shimadzu XRD-600 diffractometer, with Cu Kα radiation (λ = 1.5418 Å). The data were collected within a 2θ angle range of 3–40° at a scanning rate of 0.01° s^{-1}.

Synchrotron Small-Angle X-ray Scattering (SAXS). SAXS experiments (samples with 7 mm of the diameter and 1 mm thickness) were performed on the SAXS1 beamline of the Brazilian Synchrotron Light Laboratory (LNLS), monitored with a photomultiplier, and detected on a Pilatus detector (300k Dectris) positioned at 836 mm, generating scattering wave vectors (q) from 0.13 to 2.5 nm^{-1}. The wavelength of the incident X-ray beam (λ) was 0.155 nm. The samples were heated to 250°C to eliminate the thermal history and held there for 5 min, then cooled at a constant rate of 10°C min^{-1} until 30°C using Linkam DSC600 system. Background and parasitic scattering were determined by separate measurements on an empty holder and subtracted.

In this study, it was considered that the scattering objects are periodical stacks consisting of alternate lamellar crystals and amorphous layers. The detailed parameters of lamellar structures, such as long period (L_p), amorphous lamellar thickness (L_a) and crystalline lamellar thickness (L_c) can be extracted from SAXS profiles by one-dimensional correlation function, $\gamma(r)$.[33–35] Linear correlation function was determined by procedure given in the literature,[26] using Lorentz-correction SAXS intensity profiles according to the following equations:

$$\gamma(r)=\frac{\int_0^{\infty} I(q)q^2\cos(qr)dq}{\int_0^{\infty} q^2I(q)dq}=\frac{1}{Q}\int_0^{+\infty} q^2I(q)cos(qr)dq \quad (3)$$

where r is the direction perpendicular to the lamellae surfaces, along which the electron density is measured. Q is the invariant that represents the electron density difference between the two phases and has been calculated from the area under the Lorentz-corrected scattering curve. In the case of an ideal two-phase model with sharp boundaries at the crystal/amorphous

Table I. Selective Extraction, Amine End, Carboxylic Concentration Groups, Viscosity Number, and Molecular Weight of PA6/SOMA

PA6/SOMA	Selective extraction (wt %)	Amine end concentration [mol g^{-1} PA]	Carboxyl end concentration [mol g^{-1} PA]	Viscosity number (mL g^{-1})	$[\eta]$ (dL g^{-1})	M_v (g mol^{-1})
0	0.010	2.38×10^{-5}	2.69×10^{-5}	220.0	1.693	53,000
1	0.024	1.59×10^{-5}	4.09×10^{-5}	233.3	1.774	56,000
5	0.003	1.37×10^{-5}	7.54×10^{-5}	276.9	2.031	66,000

interface, the Porod's law can be given to describe the asymptotic behavior of the background-subtracted SAXS curves at the large q region.[20,36]

The lamellar structure parameters can be determined from the $\gamma(r)$ function.[37] The average crystalline thickness, L_c can be obtained by the intersection of straight line $d\gamma(r)/dr$ with the baseline at $\gamma_{min} = -A$. This baseline is defined as the horizontal tangent at the first $\gamma(r)$ minimum, which belongs to the self-correlation triangle.[35,37,38]

The long period, L_p correspond to the r value that belongs to the first $\gamma(r)$ maximum outside the self-correlation triangle. The minimal value of the long period, $L_{p\ min}$ corresponds to the double of the r value that belongs to the first $\gamma(r)$ minimum.[38] The average soft block (amorphous) thickness is determined by $L_a = L_{pmin} - L_c$. The linear correlation analysis also allows estimation of the average interface thickness between crystalline and amorphous phases using the relationship between the crystalline thickness and minimum long period, by $IT = L_c\chi_L = L_c^2/L_{pmin}$.[26,37,38]

Dynamic Mechanical Thermal Analysis (DMTA). Dynamic mechanical experiments were performed in a Netzsch DMA 242C analyzer, using three point bending geometry. Samples comprised of rectangular bars with dimensions of 40 × 10.7 × 3.2 mm were cut from the injection-molded specimens. The experiments were done within the linear viscoelastic region using small amplitude (30 μm) in the temperature range of −150 to 180°C. The heating rate was fixed at 3°C min^{-1} and the frequency was set to 1 Hz for all samples.

Capillary Rheometry. The flow behavior of the PA6/SOMA samples was measured in a capillary rheometer Rheograph 25 (Göttfert) with a capillary die of 1 mm in diameter and a L/D ratio of 30. Measurements were done at 250°C over a shear rate (γ) range between 10 and 5000 s^{-1}. The Bagley corrections have been performed with capillary dies having an L/D ratio of 30/1 and 0/1. The Rabinowitch correction and friction in the barrel were also performed.

Mechanical Properties. The tensile tests of the PA6/SOMA samples were done on type I ASTM bars using an EMIC DL 2000 universal testing machine at a crosshead speed of 50 mm min^{-1}, according to ASTM D638. The experiments were done with samples dried and hydrated for 100 h at 100% relative humidity.

RESULTS AND DISCUSSION

Table I shows the results of selective extraction, amine end, carboxylic concentration groups, viscosity number, and molecular weight. Hexane is a good solvent for soybean oil, but it is not a good solvent for polyamide due to its solubility parameter.[13] For all samples, the extraction values were practically zero. The concentration of amine end groups decreased with addition of SOMA. This is related to the reaction between the amine groups and anhydrides. The reactions between amides and anhydrides groups are commonly used in immiscible polymers blends to generate *in situ* compatibilizers[39,40]; thus, there was formation of new imides group in the samples studied. However, the concentration of carboxylic end groups increased. The literature have shown that the reaction of polyamides with anhydride species can reduce the molecular weight,[25,29,41] but may also increase the molecular weight depending on the reaction equilibrium.[21,22] When occurs a reduction in molecular weight, it was observed an increase of carboxyl groups. However, when reducing the concentration of both terminal groups there is the increasing in molecular weight.

There are different opinions about the activity of carboxylic anhydride and carboxylic acid groups towards amide groups in polyamide melt or during melt processing.[21,22,25,29] One approach deals with the reaction of carboxylic acid groups with amide groups that result in chains scission. Another approach is about reaction between amino end groups of polyamides with formation of graft copolymers. The literature has shown that not only carboxylic anhydride but also carboxylic acid groups have very high activity during polyamide melt processing. This is an alternative for the control of molecular weight during melt processing.[23,25,29] The viscosity number, intrinsic viscosity and molecular weight showed an increasing tendency with addition of SOMA, as presented in Table I. It can be inferred that the SOMA reacted with PA6, since we noted reducing amine end groups.

These reactions of chain scission and graft copolymer formation modify the acid and amine end group concentrations in polyamide. When graft copolymer formation occurs, anhydrides react with amine chain ends and consequently, the equilibrium of the polyamide is affected. Re-equilibration of the system will occur by hydrolysis, with the formation of new amine and carboxyl chain ends.[23,25,29] Maréchal and coworkers showed a good example of polyamides anhydrides with reaction mechanism.[25] The decrease of amine chain end concentration after the reaction between PA6 and SOMA is explained by the reaction with

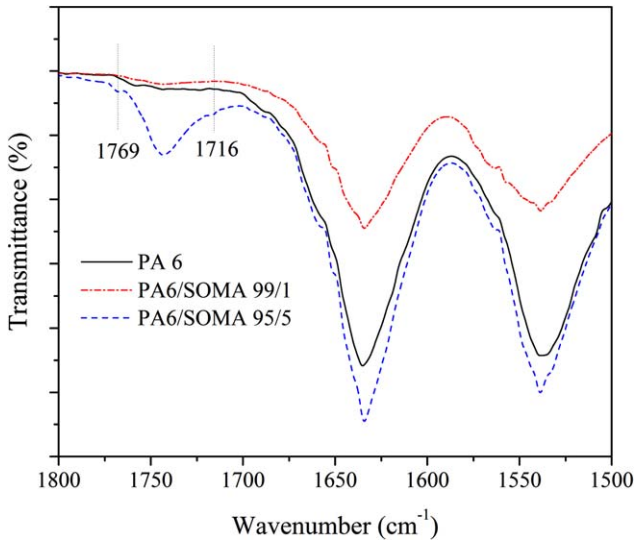

Figure 2. FTIR spectra for PA6 and PA6/SOMA blends. [Color figure can be viewed in the online issue, which is available at wileyonlinelibrary.com.]

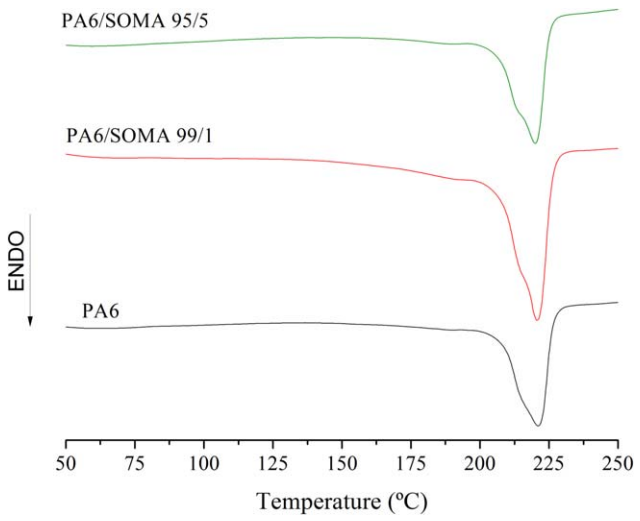

Figure 3. DSC thermographs for second heating cycle. [Color figure can be viewed in the online issue, which is available at wileyonlinelibrary.com.]

anhydride groups, while the increase of carboxyl chain end concentration and the increase of the PA6 molecular weight are explained by the free acid groups of SOMA generated during the melt processing by scission of triglyceride molecules and formation of free fatty acids.[42]

After reaction with SOMA, the FTIR spectra of the samples (Figure 2) presented three new absorption bands at 1769, 1742, and 1716 cm^{-1}. The 1773 and 1717 cm^{-1} bands are mainly related from the symmetric and antisymmetric carbonyl stretching mode of the cyclic aromatic imide groups.[25,29] The intensity in 1742 cm^{-1} is associated with the C═O in triacylglycerol molecules.[3]

Figure 3 shows the DSC thermograms (second heating curves). Addition of SOMA did not significantly affect the melting point of PA6 (T_m close to 220°C).[24,43] Nevertheless, the addition of SOMA promoted the formation of a shoulder in the melting peak. This shoulder is related to the melting of the γ crystalline phase of PA 6, which shows melting temperature of 214°C, while the α crystalline phase shows a melting point at 220°C.[44–46]

Table II shows the DSC results for the melting points (T_{m1} and T_{m2}) and fusion enthalpies (ΔH_{m1} and ΔH_{m2}) for first (1) and second (2) heating cycles; the crystallization temperature (T_c) and crystallization enthalpy (ΔH_c); and the crystallinity index (X_c) determined from ΔH_{m2}, based on the fusion enthalpy of a purely crystallinity forms of PA 6 (ΔH_f^0). Because ΔH_f^0 values of the two crystalline forms (α and γ forms) were nearly identical, 241 J g^{-1} for α and 239 J g^{-1} for the γ form.[47,48] In this work, the average value of two crystalline forms (240 J g^{-1}) were used to calculate the crystallinity index, according to procedure used by Baldi and coworkers.[49] Incorporation of SOMA did not modify the melting temperatures (T_{m1} and T_{m2}); the crystallization temperature had a small decreasing with the addition of 5 wt % SOMA. The sample PA6/SOMA99/1 had highest ΔH_m and ΔH_c values, indicating an increase in crystallinity for this sample.

Addition of SOMA increased the local mobility of PA6 because the soybean oil viscosity is much lower than PA6 viscosity during crystallization. Nevertheless, the results exposed that most of the anhydride reacted, and it was not possible to extract the oil from the PA6.

The WAXD diffractograms for the samples are shown in Figure 4. It was observed an intense peak at 21.1°, related to the diffraction of (001) plane from γ phase.[50,51] The sample PA6/SOMA95/5 showed other two peaks, one at 20.1°, related to (200) plane from α phase, and other peak at 23.1°, associated with (202) and (002) planes from α phase.[51] Therefore, addition of SOMA increased the amount of α phase.

Figure 5 shows the results for long lamellar period (L_p), average amorphous layer thickness (L_a), and average crystalline layer

Table II. Melting Points, Fusion Enthalpies for First and Second Heating Cycles; Crystallization Temperature (T_c), Crystallization Enthalpy (ΔH_c); and the Crystallinity Index (X_c) for PA6/SOMA Blends

Sample	T_{m1} (°C); ΔH_{m1} (J g^{-1})	T_c (°C); ΔH_c (J g^{-1})	T_{m2} (°C); ΔH_{m2} (J g^{-1})	X_c (%)
PA6	221.2; 53.9	184.7; 63.4	221.1; 64.3	26.8
PA6/SOMA 99/1	223.5; 65.5	184.3; 87.6	220.7; 88.5	36.8
PA6/SOMA 95/5	220.2; 54.1	182.9; 65.0	220.0; 67.3	28.0

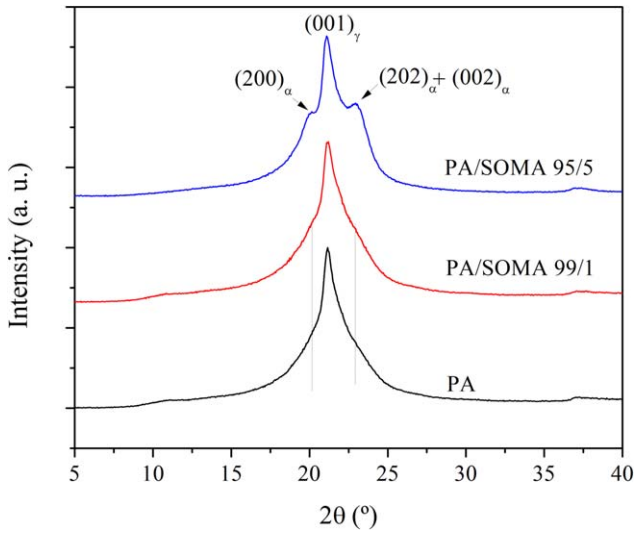

Figure 4. WAXD results. [Color figure can be viewed in the online issue, which is available at wileyonlinelibrary.com.]

thickness (L_c) as function of temperature. These parameters were obtained from the linear correlation functions $\gamma(r)$ [eq. (3)]. The L_p values observed were similar to the one found in literature.[52] The decrease in temperature promoted a reduction in L_p, as expected. Addition of SOMA did not affect the L_p size, since SOMA molecules have significant size as well as low solubility in PA6, what segregates SOMA molecules from the crystalline region. Addition of small molecules in PA6, such as water, can increase the lamellar structure in up to 5% its original size.[53]

Both L_a and L_c values showed a reduction tendency with the decreasing of temperature. The average amorphous layer thickness (L_a) had no influence of SOMA between 190 and 140°C. However, in the range 140–30°C, it was observed higher L_a values for the sample PA6/SOMA99/1. The average crystalline layer thickness (L_c) was significantly dependent on SOMA content. The neat PA6 had the lower values for L_c in all temperature range evaluated.

Polyamides with branches presented reduction in viscosity,[22] due to this reason increases the mobility of polymer. Since SOMA have lower viscosity than PA6 at the temperature in which crystallization starts, addition of SOMA reduces the local viscosity and promotes higher L_c values (thicker crystalline domains). At 190°C, the addition of 5 wt % SOMA promoted and increase of L_c from 3.36 (neat PA6) to 3.66 nm (approximately 9%). SOMA reacted predominantly at the PA6 chain ends, and these regions are excluded from the crystalline growth front. Generally, there is a balance between the increase in the crystalline and amorphous regions sizes, and L_p values remain unchanged. The size of the crystalline block (L_c) rises due to the increasing mobility by reaction with SOMA. Hence, a greater amount of chains can form ordered regions having sufficient mobility in the crystallization temperature. This trend corroborates with the results found in DSC measurements.

The size of the interfacial region amorphous/crystalline phases increased from 1.23 nm (neat PA6) to 1.31 nm (PA6/SOMA99/1) and 1.33 nm (PA6/SOMA95/5). These results suggested that SOMA molecules are located at the interfacial region, increasing its size.

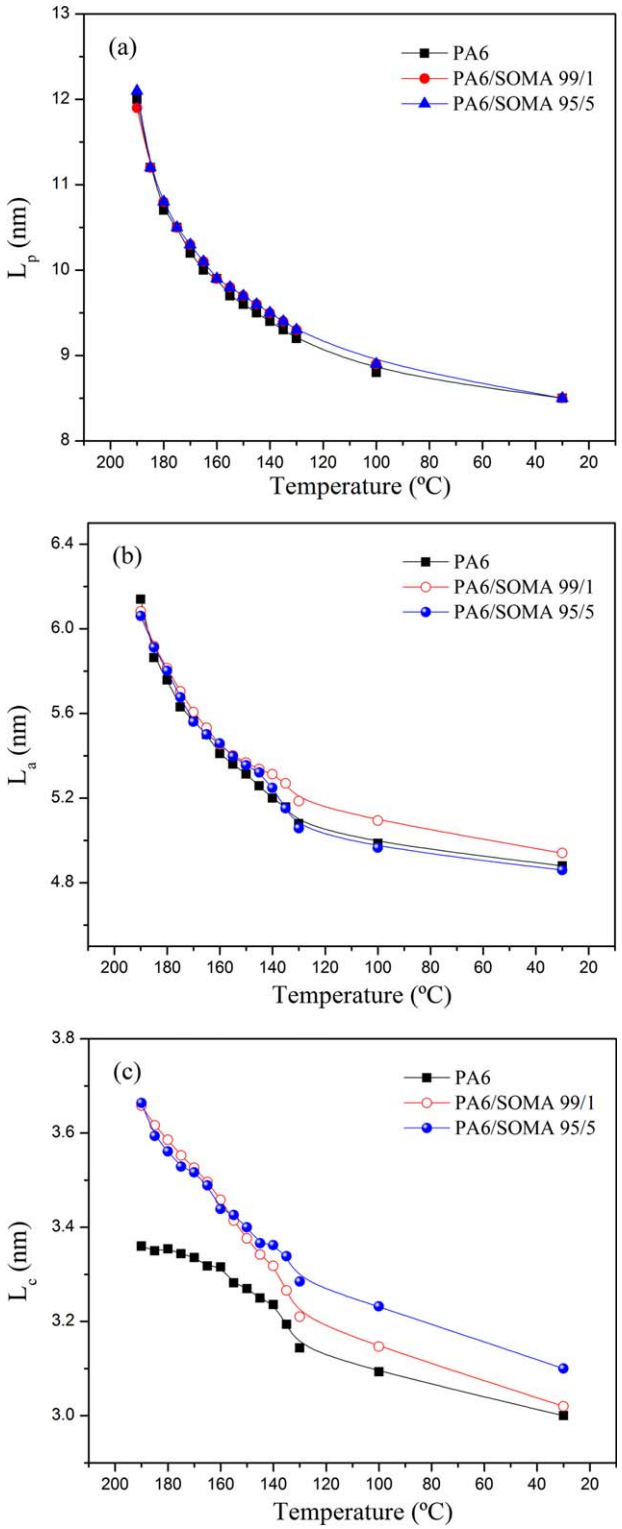

Figure 5. SAXS parameters in function of temperature: (a) long lamellar period (L_p); (b) average amorphous layer thickness (L_a); (c) average crystalline layer thickness (L_c). [Color figure can be viewed in the online issue, which is available at wileyonlinelibrary.com.]

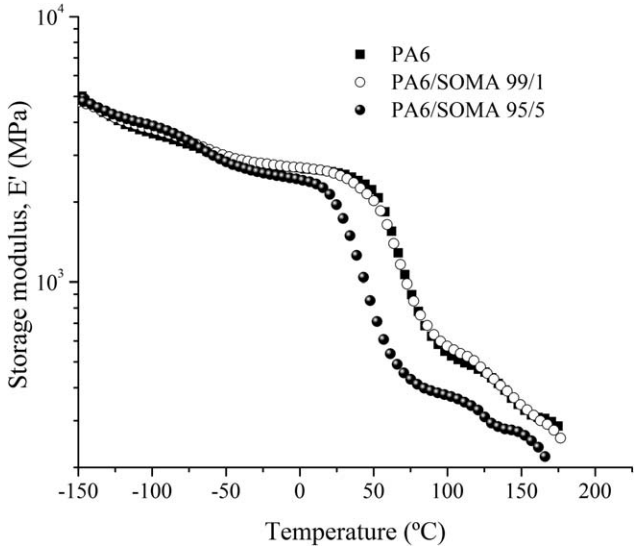

Figure 6. Storage modulus (E') for PA6 and PA6/SOMA blends.

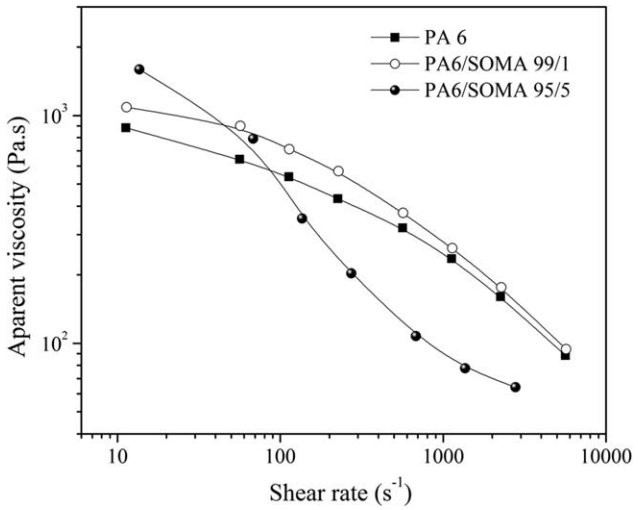

Figure 8. Apparent viscosity versus shear rate (γ) for PA6 and PA6/SOMA blends.

The dynamic mechanical properties, storage modulus (E'), and damping factor (tan δ) of pure PA 6 and PA6/SOMA blends are shown in Figures 6 and 7, respectively. All samples showed a solid-like behavior throughout the temperature range evaluated. PA6/SOMA 95/5 presented smaller E' values than the other samples at temperatures above 25°C. This is due to the increased molecular mobility caused by the addition of SOMA.

From Figure 7, it was observed that PA6 had three relaxations peaks, observed at approximately 72, −63, and −134°C, which are referred to as α, β, and γ relaxation transitions temperatures of PA6, respectively.[54] The α relaxation peak is related to the breakage of hydrogen bonds between polymer chain (CONH groups), which induces long range segmental chain movement in the amorphous area. This is assigned to the glass transition temperature of PA6. The β relaxation is related to segmental motion involving amide groups that are not H-bonded to other amide groups. The γ peak reflects the onset of cooperative motions of CH_2 groups between amide linkages in the amorphous fractions.[24] The addition of 5 wt % of SOMA resulted in a reduction of α transition, which is related to the reduction of the hydrogen bonds density. Other relaxations were not altered by the addition of SOMA.

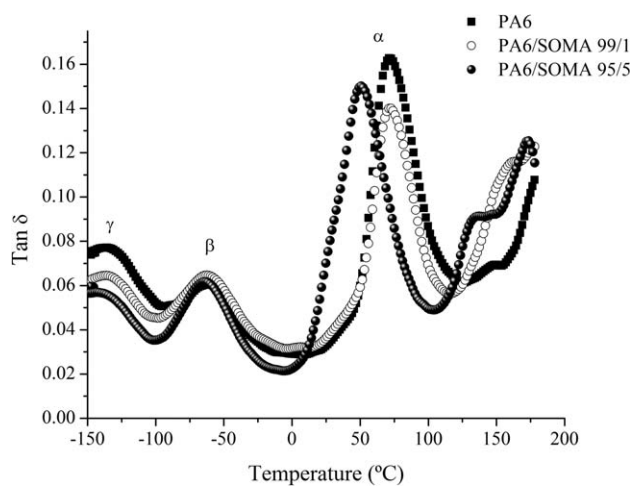

Figure 7. Damping factor (tan δ) for PA6 and PA6/SOMA blends.

Figure 8 shows apparent viscosity as a function of shear rate for the PA 6 and PA6/SOMA blends. One can observe that the addition of 1 wt % of SOMA promoted only a small rise in viscosity profile, related to the increase in molecular weight due to the addition of SOMA molecules to the PA through covalent linkages. The pseudoplastic behavior for samples PA6 and PA6/SOMA 99/1 were similar. However, the PA6/SOMA 95/5 sample showed a more marked pseudoplastic behavior, having a higher apparent viscosity at low shear rates, and a more pronounced decrease in viscosity with the increase in shear rate. The addition of 5 wt % SOMA to the polyamide chains apparently facilitates the disentanglement and alignment of molecules under

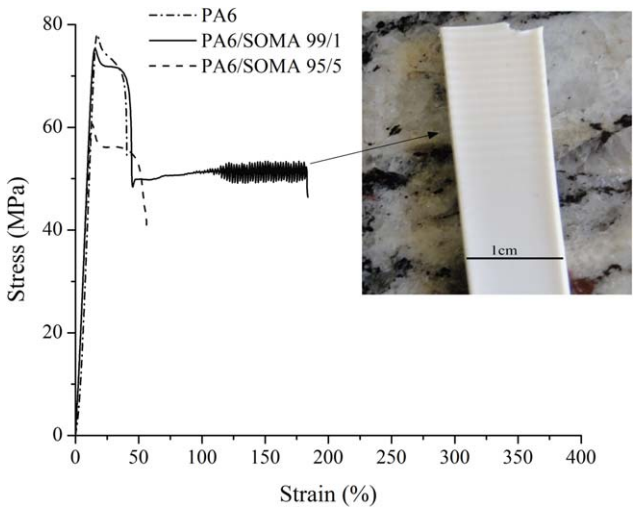

Figure 9. Stress versus strain for dried PA6 and PA6/SOMA blends. [Color figure can be viewed in the online issue, which is available at wileyonlinelibrary.com.]

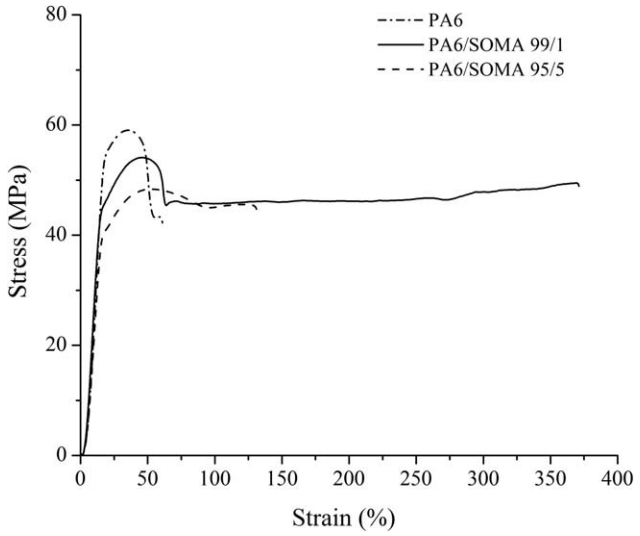

Figure 10. Stress versus strain for hydrated PA6 and PA6/SOMA blends.

flow, reducing the apparent viscosity. This is related to the increasing in free volume caused by star shape structure of the SOMA.

Figure 9 shows the results of the tensile tests for the samples dried. We observed that none significant difference occurred at the initial elastic deformation. However, the increase in SOMA content reduced the tensile strength at yield. This behavior was expected,[55] once the SOMA acted as a plasticizer reducing the glass transition temperature, as observed in the dynamic mechanical results. This trend increased the free volume and allowed the amorphous phase to deform plastically with lower stress values. The tensile results also showed that the elongation at break was increased due the addition of SOMA. A singular behavior was observed for the sample with 1 wt % of SOMA (PA6/SOMA 99/1), where the stress–strain curve had the highest deformation, as well as showed an oscillation in tension from a strain of approximately 100% until rupture. This oscillation in tension formed a "zigzag" curve, which is related to successive alignments of polymer molecules during deformation, causing successive yield points. One can expect that these yieldings are formed mainly in the crystalline domains, which were plastically deformed during strain, forming high aligned molecules and fibrillar structures.[56] The stress oscillation results in periodic fluctuation of mechanical stress in time, and is accompanied by the onset striation pattern composed of repeated transparent/opaque bands (usually crystalline), which are oriented perpendicular to the load direction.[57,58] The sample with 5 wt % of SOMA had the rupture at a lower deformation than that observed for the sample with 1 wt % of SOMA. Probably, the increase in SOMA content facilitates the rupture due to the enhancement in molecular mobility of amorphous regions. These regions deform before crystalline domains and results in rupture at small deformation.

Tensile tests for the samples hydrated for 100 h at 100% relative humidity (Figure 10) presented similar behavior as observed for the dried samples. Due to the additional plasticizer effect caused by water, the tensile strength at yield decreased and the elongation at break increased. However, the "zigzag" behavior was not observed for the samples, indicating that the presence of water molecules facilitates the alignment of the molecules and formation of fibrils, avoiding the successive yieldings. The mechanical properties of PA6/SOMA blends are summarized in Table III.

CONCLUSIONS

In this work, a soybean oil chemically modified with maleic anhydride was synthesized and melt reacted with polyamide 6. The incorporation of SOMA into PA6 promoted an increasing in viscosimetric molecular weight. FTIR measurements, extraction and titration experiments showed that nearly all SOMA molecules were covalently bonded to PA6, making difficult the extraction and, consequently, avoiding additive surface migration. The SOMA did not considerably affect the melting point of PA6 as showed by DSC curves; however, the addition of 1 wt.% significantly improved the relative crystallinity of PA6. This trend lead to a material with much higher tenacity and elongation at break compared to pure PA6, both in dry or in 100% relative humidity conditions.

SAXS measurements showed that incorporation of SOMA did not affect the L_p size, since SOMA molecules have significant size as well as low solubility in PA6. The average crystalline layer thickness (L_c) was significantly dependent on SOMA content. The average amorphous layer thickness (L_a) was increased with the addition of 1 wt % of SOMA, while the average crystalline layer thickness (L_c) was significantly enlarged with the increase in SOMA content. This trend indicated that SOMA structures were located at the interfacial region between amorphous and crystalline. DMA measurements indicated that only the glass transition temperature was affected by the addition of SOMA. The T_g had a reduction with the incorporation of 5 wt %. This decreasing of T_g designates a plasticizing effect induced by SOMA. Capillary rheology measurements revealed that the pseudoplastic behavior for samples PA6 and PA 6/SOMA 99/1

Table III. Mechanical Properties of PA6/SOMA Blends

	Tensile strength (MPa)		Elongation at break (%)		Toughness (J)	
Sample	Dry	Hydrated	Dry	Hydrated	Dry	Hydrated
PA6	77.9 ± 7.0	59.1 ± 3.5	25.9 ± 3.6	60.9 ± 5.2	50.9 ± 9.8	67.0 ± 8.4
PA6/SOMA 99/1	75.5 ± 3.2	53.9 ± 2.7	88.0 ± 29.8	278.2 ± 102.8	144.2 ± 46.3	261.4 ± 98.9
PA6/SOMA 95/5	67.0 ± 2.7	48.4 ± 0.2	42.0 ± 22.6	131.0 ± 12.7	69.2 ± 5.9	121.1 ± 12.3

were similar. Nevertheless, the PA 6/SOMA 95/5 sample exhibited a more noticeable pseudoplastic behavior when compared to the other samples. This indicates that SOMA addition increased the free volume of polyamide 6.

The PA6/SOMA had very interesting properties regarding tenacity, elongation at break, and crystallinity. This study proved that a modified additive from renewable source can improve PA6 properties leading to a material that can be used in new application possibilities.

ACKNOWLEDGMENTS

The authors are thankful to Mantova Ltd. for donation of the polyamide, CAPES, and CNPq for financial support and the Brazilian Synchrotron Light Laboratory (LNLS) for SAXS analyses (SAXS1 beamline). The authors would like to thank Prof. Dr. Robinson D. Cruz for the supporting in the capillary rheometry analysis.

REFERENCES

1. Fiorio, R.; Zattera, A. J.; Ferreira, C. A. *Polym. Eng. Sci.* **2010**, *50*, 2321.
2. Fiorio, R.; Zattera, A. J.; Ferreira, C. A. *J. Appl. Polym. Sci.* **2009**, *112*, 2896.
3. Ourique, P. A.; Gril, J. M. L.; Guillaume, G. W.; Wanke, C. H.; Echeverrigaray, S. G.; Bianchi, O. *J. Appl. Polym. Sci.* **2015**, *132*.
4. Gandini, A.; Lacerda, T. M. *Prog. Polym. Sci.* **2015**, *48*, 1.
5. Gujel, A. A.; Bandeira, M.; Giovanela, M.; Carli, L. N.; Brandalise, R. N.; Crespo, J. S. *Mater. Des.* **2014**, *53*, 1119.
6. Gujel, A. A.; Bandeira, M.; Veiga, V. D.; Giovanela, M.; Carli, L. N.; Mauler, R. S.; Brandalise, R. N.; Crespo, J. S. *Mater. Des.* **2014**, *53*, 1112.
7. Schiller, M. PVC Additives; Carl Hanser Verlag: München, **2013**.
8. Henkel AG and Tecnaro. GmbH Additives for Polymers, **2011**, *2011*, p 2.
9. Lardjane, N.; Belhaneche-Bensemra, N.; Massardier, V. *J. Polym. Res.* **2013**, *20*, 1.
10. Greco, R.; Lanzetta, N.; Maglio, G.; Malinconico, M.; Martuscelli, E.; Palumbo, R.; Ragosta, G.; Scarinzi, G. *Polymer* **1986**, *27*, 299.
11. Gu, H.; Guo, Y.; Wong, S. Y.; Zhang, Z.; Ni, X.; Zhang, Z.; Hou, W.; He, C.; Shim, V. P. W.; Li, X. *Micropor. Mesopor. Mater.* **2013**, *170*, 226.
12. Krause, B.; Schneider, C.; Boldt, R.; Weber, M.; Park, H. J.; Pötschke, P. *Polymer* **2014**, *55*, 3062.
13. van Krevelen, D. W.; te Nijenhuis, K. Properties of Polymers: Their Correlation with Chemical Structure; Their Numerical Estimation and Prediction from Additive Group Contributions; Elsevier Science: New York, **2009**.
14. Liu, C.; Li, J.; Lei, W.; Zhou, Y. *Indus. Crops Prod.* **2014**, *52*, 329.
15. Xiong, Z.; Li, C.; Ma, S.; Feng, J.; Yang, Y.; Zhang, R.; Zhu, J. *Carbohydr. Polym.* **2013**, *95*, 77.
16. Tran, P.; Seybold, K.; Graiver, D.; Narayan, R. *J. Am. Oil Chem. Soc.* **2005**, *82*, 189.
17. Eren, T.; Küsefoğlu, S. H.; Wool, R. *J. Appl. Polym. Sci.* **2003**, *90*, 197.
18. Xanthos, M. Reactive Extrusion: Principles and Practice; Hanser Publishers: Munich, **1992**.
19. Raquez, J. M.; Degée, P.; Nabar, Y.; Narayan, R.; Dubois, P. *Comp. Rendus Chim.* **2006**, *9*, 1370.
20. Bianchi, O.; Barbosa, L. G.; Machado, G.; Canto, L. B.; Mauler, R. S.; Oliveira, R. V. B. *J. Appl. Polym. Sci.* **2013**, *128*, 811.
21. Schacker, O.; Braun, D.; Hellmann, G. P. *Macromol. Mater. Eng.* **2001**, *286*, 382.
22. Coltelli, M. B.; Angiuli, M.; Passaglia, E.; Castelvetro, V.; Ciardelli, F. *Macromolecules* **2006**, *39*, 2153.
23. Lehmann, D. In Polymers-Opportunities and Risks II; Springer: New York, **2010**.
24. Kohan, M. I.; Kohan, M. I. Nylon Plastics Handbook; Hanser/Gardner Publications: Cincinnati, **1995**.
25. Maréchal, P.; Coppens, G.; Legras, R.; Dekoninck, J. M. *J. Polym. Sci. A: Polym. Chem.* **1995**, *33*, 757.
26. Carli, L. N.; Bianchi, O.; Machado, G.; Crespo, J. S.; Mauler, R. S. *Mater. Sci. Eng. C* **2013**, *33*, 932.
27. Bondan, F.; Soares, M. F.; Bianchi, O. *Polym. Bull.* **2014**, *71*, 151.
28. Bondan, F.; Bianchi, O. *Sci. cum Indus.* **2015**, *3*, 23.
29. Eichhorn, K. J.; Lehmann, D.; Voigt, D. *J. Appl. Polym. Sci.* **1996**, *62*, 2053.
30. Lu, C.; Chen, T.; Zhao, X.; Ren, X.; Cai, X. *J. Polym. Sci. B: Polym. Phys.* **2007**, *45*, 1976.
31. Solomon, O. F.; Ciută, I. Z. *J. Appl. Polym. Sci.* **1962**, *6*, 683.
32. Bianchi, O.; Repenning, G. B.; Mauler, R. S.; Oliveira, R. V. B.; Canto, L. B. *Polímeros* **2012**, *22*, 125.
33. Albrecht, T.; Strobl, G. *Macromolecules* **1996**, *29*, 783.
34. Denchev, Z.; Nogales, A.; Ezquerra, T. A.; Fernandes-Nascimento, J.; Baltà-Calleja, F. J. *J. Polym. Sci. B: Polym. Phys.* **2000**, *38*, 1167.
35. Sun, Y. S. *Polymer* **2006**, *47*, 8032.
36. Cardoso, M. B.; Westfahl, Jr., H. *Carbohydr. Polym.* **2010**, *81*, 21.
37. Fatnassi, M.; Ben Cheikh Larbi, F.; Halary, J. L. *Int. J. Polym. Sci.* **2010**, *2010*.
38. Fatnassi, M.; Larbi Fadhel Ben, C.; Dubault, A.; Halary Jean, L. *e-Polymers* **2005**, *5*, 585.
39. Rösch, J.; Mülhaupt, R. In Toughened Plastics II- Novel Approaches in Science and Engineering; Riew, C. K.; Kinloch, A. J., Eds.; American Chemical Society: Washington DC, **1996**, *2*, p 291.
40. Rösch, J.; Mülhaupt, R. In Toughened Plastics II; American Chemical Society: USA, **1996**; Chapter 19.
41. Eyerer, P. Polymers: Opportunities and Risks I: General and Environmental Aspects; Springer: New York, **2010**.

42. Crossley, A.; Heyes, T. D.; Hudson, B. J. F. *J. Am. Oil Chem. Soc.* **1962**, *39*, 9.
43. Brandrup, J.; Immergut, E. H.; Grulke, E. A. Polymer Handbook, 2 Volumes Set; Wiley: New York, **2003**.
44. Khanna, Y. P.; Kuhn, W. P. *J. Polym. Sci. B: Polym. Phys.* **1997**, *35*, 2219.
45. Penel-Pierron, L.; Depecker, C.; Seguela, R.; Lefebvre, J. M. *J. Polym. Sci. B: Polym. Phys.* **2001**, *39*, 484.
46. Liu, Y.; Yang, G. *Thermochim. Acta* **2010**, *500*, 13.
47. Fornes, T. D.; Paul, D. R. *Polymer* **2003**, *44*, 3945.
48. Illers, K. H. *Die Makromol. Chem.* **1978**, *179*, 497.
49. Baldi, F.; Bignotti, F.; Ricco, L.; Monticelli, O.; Riccò, T. *J. Appl. Polym. Sci.* **2006**, *100*, 3409.
50. Abacha, N.; Kubouchi, M.; Sakai, T. *Exp. Polym. Lett.* **2009**, *3*, 245.
51. Konishi, R.; Ito, M. *Polymer* **2004**, *45*, 5191.
52. Wang, C.; Tsou, S. Y.; Lin, H. S. *Colloid Polym. Sci.* **2012**, *290*, 1799.
53. Laurati, M.; Arbe, A.; Rios de Anda, A.; Fillot, L. A.; Sotta, P. *Polymer* **2014**, *55*, 2867.
54. Serpe, G.; Chaupart, N. *J. Polym. Sci. B: Polym. Phys.* **1996**, *34*, 2351.
55. Vieira, M. G. A.; da Silva, M. A.; dos Santos, L. O.; Beppu, M. M. *Eur. Polym. J.* **2011**, *47*, 254.
56. Harrison, I. R. *J. Polym. Sci. Polym. Lett. Ed.* **1974**, *12*, 603.
57. García Gutiërrez, M. C.; Karger-Kocsis, J.; Riekel, C. *Chem. Phys. Lett.* **2004**, *398*, 6.
58. Karger-Kocsis, J.; Shang, P. P. *J. Therm. Anal. Calorim.* **2002**, *69*, 499.